

MARTIN MARIETTA ENERGY SYSTEMS LIBRARIES



3 4456 0375989 5

34

**oml**

ORNL/TM-12347

**OAK RIDGE  
NATIONAL  
LABORATORY**

**MARTIN MARIETTA**

**The Fourier  
Analysis Technique and  
Epsilon-Pseudo-Eigenvalues**

June M. Donato

OAK RIDGE NATIONAL LABORATORY

CENTRAL RESEARCH LIBRARY

CIRCULATION SECTION

4900N ROOM 175

**LIBRARY LOAN COPY**

DO NOT TRANSFER TO ANOTHER PERSON

If you wish someone else to see this  
report, send in name with report and  
the library will arrange a loan.

UCR-10044-874

MANAGED BY  
MARTIN MARIETTA ENERGY SYSTEMS, INC.  
FOR THE UNITED STATES  
DEPARTMENT OF ENERGY

This report was prepared as an account of work sponsored by an agency of the United States Government. Neither the United States Government nor any agency thereof, nor any of their employees, makes any warranty, express or implied, or assumes any legal liability or responsibility for the accuracy, completeness, or usefulness of any information, apparatus, product, or process disclosed, or represents that its use would not infringe privately owned rights. Reference herein to any specific commercial product, process, or service by trade name, trademark, manufacturer, or otherwise, does not necessarily constitute or imply its endorsement, recommendation, or favoring by the United States Government or any agency thereof. The views and opinions of authors expressed herein do not necessarily state or reflect those of the United States Government or any agency thereof.

This report has been reproduced directly from the best available copy.

Available to DOE and DOE contractors from the Office of Scientific and Technical Information, P.O. Box 62, Oak Ridge, TN 37831; prices available from (615) 576-8401, FTS 626-8401.

Available to the public from the National Technical Information Service, U.S. Department of Commerce, 5285 Port Royal Rd., Springfield, VA 22161.

ORNL/TM-12347

Engineering Physics and Mathematics Division

Mathematical Sciences Section

405  
32

**THE FOURIER ANALYSIS TECHNIQUE AND  
EPSILON-PSEUDO-EIGENVALUES**

June M. Donato

Mathematical Sciences Section  
Oak Ridge National Laboratory  
P.O. Box 2008, Bldg. 6012  
Oak Ridge, TN 37831-6367

Date Published: July 1993

Research was supported by the Applied Mathematical Sciences Research Program of the Office of Energy Research, U.S. Department of Energy.

Prepared by the  
Oak Ridge National Laboratory  
Oak Ridge, Tennessee 37831  
managed by  
Martin Marietta Energy Systems, Inc.  
for the  
U.S. DEPARTMENT OF ENERGY  
under Contract No. DE-AC-05-84OR21400



3 4456 0375989 5



# THE FOURIER ANALYSIS TECHNIQUE AND EPSILON-PSEUDO-EIGENVALUES

June M. Donato

## Abstract

The spectral radii of iteration matrices and the spectra and condition numbers of preconditioned systems are important in forecasting the convergence rates for iterative methods. Unfortunately, the spectra of iteration matrices or preconditioned systems is rarely easily available. The Fourier analysis technique has been shown to be a useful tool in studying the effectiveness of iterative methods by determining approximate expressions for the eigenvalues or condition numbers of matrix systems.

For non-symmetric matrices the eigenvalues may be highly sensitive to perturbations. The spectral radii of nonsymmetric iteration matrices may not give a numerically realistic indication of the convergence of the iterative method. Trefethen and others have presented a theory on the use of  $\epsilon$ -pseudo-eigenvalues in the study of matrix equations.

For Toeplitz matrices, we show that the theory of  $\epsilon$ -pseudo-eigenvalues includes the Fourier analysis technique as a limiting case. For non-Toeplitz matrices, the relationship is not clear. We shall examine this relationship for non-Toeplitz matrices that arise when studying preconditioned systems for methods applied to a two-dimensional discretized elliptic differential equation.



## 1. Introduction

The spectral radii of iteration matrices and the spectra and condition numbers of preconditioned systems are important in forecasting the convergence rates of iterative methods. A variety of methods are used in the analysis of such matrices [1,12,13,19].

It is not always possible to determine analytic formulas describing the eigenvalues of a given matrix. Similarly, it is not always possible to determine reasonable analytic bounds on the extremal eigenvalues or the condition number of a matrix. In many cases where bounds have been determined, the analysis has been difficult or tedious [2,9].

When exact eigenvalue analysis is used to obtain extremal eigenvalue bounds, we must be aware that for non-normal matrices that these eigenvalues can be highly sensitive to perturbations. Hence, the exact spectral radius or condition number of a non-normal iteration matrix may not give a realistic indication of the usefulness of the iterative method or preconditioner.

Motivated by the sensitivity of the eigenvalues to perturbations in the matrix, Trefethen and others have utilized a theory on  $\epsilon$ -pseudo-eigenvalues in the study of matrix equations. The  $\epsilon$ -pseudo-eigenvalues of non-normal matrices may portray radically different qualities than the exact eigenvalues for the matrix. See references [15] and [18].

Alternately, a heuristic technique based on Fourier analysis can be used to easily obtain eigenvalue approximations. The technique has been shown to be a useful heuristic when studying the effectiveness of iterative methods and preconditioners [3,5,6,7,8,10]. As yet no rigorous explanation of why this technique works so well for non-periodic non-constant diagonal matrices has been established. For symmetric Toeplitz matrices, the technique yields the true eigenvalue expressions, but it does not always yield a good approximation for general matrices.

Herein, it is shown that for Toeplitz matrices the theory of  $\epsilon$ -pseudo-eigenvalues includes the Fourier analysis technique as a limiting case. Hence, the Fourier approximate eigenvalues serve as an approximation to the  $\epsilon$ -pseudo-eigenvalues.

For non-Toeplitz matrices, the relationship is not clear. Here, we consider non-Toeplitz matrices that arise when studying preconditioned systems for methods applied to a two-dimensional discretized elliptic differential equation. We examine the relationship between the Fourier approximate eigenvalues and the  $\epsilon$ -pseudo-eigenvalues for these matrices.

The remainder of this paper is organized as follows. In Sections 2 and 3 we very briefly overview the Fourier analysis technique and concepts from the theory of  $\epsilon$ -pseudo-eigenvalues, respectively. For greater detail and a wide range of examples and applications see the references, especially [6,15,18]. In Section 4 we present the theorem linking the Fourier analysis technique and  $\epsilon$ -pseudo-eigenvalues for Toeplitz matrices. In Section 5 the spectra, Fourier approximate eigenvalues, and the  $\epsilon$ -pseudo-eigenvalues are graphically presented for a variety of Toeplitz matrices. In Section 6 we examine the relationship between the Fourier analysis technique and  $\epsilon$ -pseudo-eigenvalues by comparing results for preconditioned systems for a discretized two-dimensional elliptic partial differential equation. In Section 7 results and observations are summarized.

Derivations of the Fourier approximate eigenvalues expressions are given in an appendix.

## 2. Fourier Analysis

Fourier analysis is a pervasive subject in all of mathematics. Here we are interested in how it can be used to determine eigenvalues or approximate eigenvalues of a given matrix. Consider a one-dimensional constant coefficient elliptic partial differential equation (PDE) with periodic boundary conditions discretized on a uniform grid with  $N$  internal grid points. Let  $Au = b$  denote the resulting matrix system where  $A$  is an  $(N + 1) \times (N + 1)$  matrix.

Let  $u^{(s)}$  be a column vector of length  $N + 1$  composed of the one-dimensional Fourier exponential modes.<sup>1</sup> The  $j^{\text{th}}$  component of  $u^{(s)}$  is given by

$$u_j^{(s)} = e^{ij\theta_s} \text{ where } \theta_s = \frac{2\pi s}{N + 1}, \quad j = 0, 1, \dots, N, \quad s = 0, 1, \dots, N.$$

The  $N + 1$  vectors  $\{u^{(s)} : s = 0, 1, \dots, N\}$ , called the *Fourier vectors*, are eigenvectors of such a circulant matrix  $A$ . The fact that we know a basis for such a matrix makes it quite easy to determine an analytic formula for its eigenvalues.

Although elliptic PDEs rarely yield circulant matrices when discretized, Fourier analysis is often used [5,6,7,8] in the same way that von Neumann analysis is used for time-dependent systems [16], and local mode analysis is used for multigrid methods [4].

The steps of the Fourier analysis technique as given by [6] for an elliptic partial differential equation are summarized as follows:

- (a) Treat the matrices involved as if they came from periodic problems. This may involve ignoring the original boundary conditions of the problem and/or extending the original matrix.
- (b) Force the matrices to have constant diagonal entries. This may entail using an asymptotic value for the diagonal entries, as in the case for the ILU preconditioner.
- (c) From concepts developed in [6] use the relation  $h_p = 2h_d$  to relate the periodic mesh size to the Dirichlet mesh size.

After performing the above steps, we would have a circulant matrix whose eigenvectors are the Fourier vectors of the appropriate dimension. We are then able to use exact Fourier analysis on the altered matrix to determine approximations of its minimum or maximum eigenvalues or to observe the general shape of its spectrum. This is done simply by computing

$$\tilde{A}u^{(s)} = \tilde{\lambda}_s u^{(s)},$$

---

<sup>1</sup>Similarly, for a constant coefficient matrix with Dirichlet or Neumann boundary conditions we would use the Fourier sine or cosine modes, respectively, as eigenvector components.

where  $\tilde{A}$  represents the modified matrix and  $\tilde{\lambda}_s$  denotes the  $s^{\text{th}}$  eigenvalue of  $\tilde{A}$ . Since  $\tilde{A}$  is constant diagonal, this computation can be done easily using component or stencil form. The eigenvalue,  $\tilde{\lambda}_s$ , is a function of  $\theta_s^{(p)} = 2\pi sh_p = 2\pi s/(n_p + 1)$  where  $n_p = 2n_d + 1$  and  $s \in \{1, \dots, n_p\}$ . Thus,  $\theta_s^{(p)} \in (0, 2\pi)$ .

The *Fourier approximate eigenvalues* of  $A$ ,  $\hat{\Lambda}$ , are then given by the eigenvalues of  $\tilde{A}$ :

$$\hat{\lambda}_s = \hat{\lambda}_s(A) = \tilde{\lambda}_s.$$

The degenerate eigenvalue,  $\tilde{\lambda}_s = 0$ , is ignored when doing analysis for a problem with Dirichlet boundary conditions.

For higher dimensional problems, the same steps as given above would be followed to generate the approximating matrix  $\tilde{A}$ . However, the appropriate dimensioned Fourier modes would form the components of the eigenvectors of  $\tilde{A}$ . For example, suppose we have a two-dimensional problem discretized on a uniform grid with  $N$  internal grid points in each direction. Then the Fourier  $(j, k)^{\text{th}}$  component of the  $(s, t)^{\text{th}}$  eigenvector would be given by

$$u_{j,k}^{(s,t)} = e^{ij\theta_s} e^{ik\phi_t}, \quad 0 \leq s, t \leq n,$$

where  $\theta_s = 2\pi sh$ ,  $\phi_t = 2\pi th$ ,  $h = 1/(n + 1)$ . As above, we would then determine  $\tilde{\lambda}_{s,t}$  from

$$\tilde{A}u^{(s,t)} = \tilde{\lambda}_{s,t}u^{(s,t)}.$$

As in the one-dimensional case, the singular cases with  $s = 0$  or  $t = 0$  are ignored in the analysis of problems with Dirichlet boundary conditions.

### 3. $\epsilon$ -pseudo-eigenvalues

For non-hermitian matrices, the eigenvalues of the matrix may be highly sensitive to perturbations. Hence, when analyzing a matrix to determine its behavior as an iteration matrix or as a preconditioner, the true eigenvalues of the matrix may be misleading. In fact, we are more interested in the behavior of the eigenvalues when the matrix  $A$  is perturbed.

This is the connection to the theory of  $\epsilon$ -pseudo-eigenvalues as presented in references [15,17,18]. There are several theoretically equivalent definitions for  $\epsilon$ -pseudo-eigenvalues. We will use the following definition from [18].

**DEFINITION:** Given  $\epsilon > 0$ ,  $\lambda \in \mathbf{C}$  is an  $\epsilon$ -pseudo-eigenvalue of the  $N \times N$  matrix  $A$  if  $\lambda$  is an eigenvalue of  $A + E$  for some  $E \in \mathbf{C}^{N \times N}$  with  $\|E\| \leq \epsilon$ . The set of all  $\epsilon$ -pseudo-eigenvalues of  $A$ , called the  $\epsilon$ -pseudo-spectrum, is denoted  $\Lambda_\epsilon(A)$  or simply  $\Lambda_\epsilon$ .

Rather than examine the exact eigenvalues of a non-normal matrix  $A$  we want to examine  $\Lambda_\epsilon$ . However, computing  $\Lambda_\epsilon(A)$  using the definition is not always desirable or feasible for large  $N$ . But, Reichel and Trefethen [15] have observed a relationship between the  $\epsilon$ -pseudo-spectrum and the union of three sets for Toeplitz matrices. The following is an overview of one of their results.

Consider the matrix problem  $Au = b$  where  $A$  is a Toeplitz matrix

$$A = \begin{pmatrix} a_0 & a_1 & \cdots & a_N \\ a_{-1} & a_0 & \ddots & \vdots \\ \vdots & \ddots & \ddots & a_1 \\ a_{-N} & \cdots & a_{-1} & a_0 \end{pmatrix}. \quad (1)$$

A matrix of this form could have arisen from a finite-difference or finite-element discretization of a one-dimensional self-adjoint PDE. The symbol [15] of this matrix is given by  $f(z) = \sum_{k=-N}^N a_k z^k$ . The fundamental observation of [15] is that for large  $N$  and small  $\epsilon$ ,  $\Lambda_\epsilon$  looks approximately like the union of three sets:

$$\Lambda_\epsilon \simeq \Omega_r \cup \Omega^R \cup (\Lambda + \Delta_\epsilon), \quad (2)$$

where

$$\begin{aligned} \Omega_r &= \{z \in \mathbf{C} : I(f(S_r), z) > 0\} \\ \Omega^R &= \{z \in \mathbf{C} : I(f(S_R), z) < 0\} \\ S_r &= \text{circle of radius } r, r = (\epsilon/c)^{1/N} \\ S_R &= \text{circle of radius } R, R = (\epsilon/C)^{-1/N} \\ I(f, z) &= \text{winding number of } f \text{ about } z \\ \Lambda &= \text{the eigenvalues of the matrix } A \\ \Lambda + \Delta_\epsilon &= \text{union of } \epsilon\text{-balls about the eigenvalues of the matrix } A \end{aligned}$$

The values  $c$  and  $C$  [15] are generally taken to be 1.

The images of  $S_r$  and  $S_R$ ,  $f(S_r)$  and  $f(S_R)$ , are easily computed. Typically  $\Omega_r$  and  $\Omega^R$  provide a good envelope for  $\Lambda_\epsilon(A)$ . Hence, by computing the regions enclosed by  $f(S_r)$  and  $f(S_R)$ , we can get a general idea of the behavior of the matrix without the computationally expensive task of computing  $\Lambda$  or  $\Lambda_\epsilon(A)$ . This is certainly advantageous in the analysis of iterative methods and preconditioners.

#### 4. The link between the Fourier technique and $\epsilon$ -pseudo-eigenvalues

In this section it is shown that the Fourier analysis technique yields a limiting expression for the boundaries of the regions  $\Omega_r$  and  $\Omega^R$ .

**THEOREM:** For the general one-dimensional Toeplitz matrix the boundary defined by the Fourier approximate eigenvalue expression,  $\hat{\lambda}(A)$ , is a limiting case of the boundaries of  $\Omega_r$  and  $\Omega^R$  as  $r, R \rightarrow 1$ .

*Proof.* Consider again the Toeplitz matrix (1). We have already noted that the symbol of this matrix is given by

$$f(z) = \sum_{k=-N}^N a_k z^k. \quad (3)$$

From (2) we are interested in the boundaries of the regions  $\Omega_r$  and  $\Omega^R$ , which are determined by the images of  $S_r$  and  $S_R$  via the symbol  $f(z)$ . The image of  $S_r$  is given by

$$f(S_r) = \{z = f(re^{i\theta}) : \theta \in [0, 2\pi]\},$$

where

$$f(re^{i\theta}) = \sum_{k=-N}^N a_k (re^{i\theta})^k = \sum_{k=-N}^N r^k a_k (e^{i\theta})^k \quad (4)$$

with  $r = \epsilon^{1/N}$ , and similarly for  $f(S_R)$  using  $R = \epsilon^{-1/N}$  instead of  $r$ . As  $N \rightarrow \infty$ , we have  $r \rightarrow 1$ ,  $R \rightarrow 1$  since  $\epsilon \ll 1$ .

To apply the Fourier analysis technique to this Toeplitz matrix (1) we follow the steps outlined earlier. The circulant version of the matrix  $A$  is

$$\tilde{A} = \begin{pmatrix} a_0 & \cdots & a_{N-1} & a_N & a_{-N} & \cdots & a_{-1} \\ \vdots & \ddots & \vdots & \vdots & \vdots & \ddots & \vdots \\ a_N & \cdots & a_0 & a_1 & a_2 & \cdots & a_{-N} \\ a_{-N} & \cdots & a_{-1} & a_0 & a_1 & \cdots & a_N \\ \vdots & \ddots & \vdots & \vdots & \vdots & & \vdots \\ a_{-1} & \cdots & a_{-N} & a_N & a_{N-1} & \cdots & a_0 \end{pmatrix}$$

where  $\tilde{A}$  is an order  $2N + 1$  matrix.

We calculate the  $j^{\text{th}}$  component of

$$\tilde{A}u^{(s)} = \tilde{\lambda}_s u^{(s)}$$

to get

$$\begin{aligned} \tilde{A}u_j^{(s)} &= a_0 e^{ij\theta_s^{(p)}} + a_1 e^{i(j+1)\theta_s^{(p)}} + \cdots + a_N e^{i(j+N)\theta_s^{(p)}} \\ &\quad + a_{-1} e^{i(j-1)\theta_s^{(p)}} + \cdots + a_{-N} e^{i(j-N)\theta_s^{(p)}} \\ &= \left( \sum_{k=-N}^N a_k e^{ik\theta_s^{(p)}} \right) u_j^{(s)} \\ &= \tilde{\lambda}_s u_j^{(s)}. \end{aligned}$$

The Fourier approximate eigenvalues of  $A$  are then given by the eigenvalues of  $\tilde{A}$ ,

$$\hat{\lambda}_s(A) = \tilde{\lambda}_s = \sum_{k=-N}^N a_k (e^{i\theta_s^{(p)}})^k, \quad (5)$$

where  $\theta_s^{(p)} \in (0, 2\pi)$ .

By comparing the Fourier approximate eigenvalues of  $A$  in (5) to the images of  $S_r$  and  $S_R$  via the symbol for  $A$  in (4), we see that (5) is a discrete version of (4) where  $r = 1$ . And as already noted,  $r = 1$  and  $R = 1$  are the limiting values as  $N \rightarrow \infty$ . ■

Thus the theory of  $\epsilon$ -pseudo-eigenvalues includes as a limiting case the Fourier analysis technique. This result is certainly related to the fact that exact Fourier analysis leads to samples of the curve  $f(|z| = 1)$  for Toeplitz systems. In Reichel and Trefethen [15], it is stated that

For small  $\epsilon$  and large  $N$ , the  $\epsilon$ -pseudospectrum  $\Lambda_\epsilon$  of a Toeplitz matrix is roughly the same as the spectrum of the associated Toeplitz operator, namely, a region in the complex plane bounded by the curve  $f(S)$ , where  $f(z)$  is the symbol of the matrix.

The important and interesting concept here is that the theory of  $\epsilon$ -pseudo-eigenvalues may provide the explanation as to why the the approximate Fourier analysis technique has yielded good approximations even for situations where Fourier analysis does not strictly apply.

For the non-limiting case, the boundary formed by the Fourier approximate eigenvalues lies between  $\Omega_r$  and  $\Omega^R$ . And so the Fourier boundary would enclose most (if not all) of the  $\epsilon$ -pseudo-eigenvalues. Empirically, we will see that it seems to include all of the  $\epsilon$ -pseudo-eigenvalues.

## 5. Toeplitz Examples

In this section, some Toeplitz examples are given that demonstrate the relationship between  $\epsilon$ -pseudo-eigenvalues regions and the boundary defined via the Fourier approximate eigenvalues. In these examples, we use  $N = 100$  for the order of the matrix  $A$  and  $\epsilon = 10^{-4}$ . First, we consider two Toeplitz matrices studied in [15]. After these examples, we consider Toeplitz matrices arising from the discretization of a one-dimensional second-order differential equation.

In each of these pictures, the true eigenvalues, the  $\epsilon$ -pseudo-eigenvalues using a set of five randomly generated perturbation matrices,  $f(S_r)$ ,  $f(S_R)$ , and the Fourier approximate eigenvalues are plotted. See the legend given in Table 1.

In each of these pictures we see that the  $\epsilon$ -pseudo-eigenvalues are enclosed by  $\Omega^R$ , which is surrounded by the Fourier boundary.

In Figure 1, example (3.8) of [15] is plotted along with the Fourier approximate

eigenvalues. The matrix is

$$A = \begin{pmatrix} 0 & 2 & & & \\ 1 & \ddots & \ddots & & \\ & \ddots & \ddots & 2 & \\ & & & 1 & 0 \end{pmatrix}. \quad (6)$$

In Figure 1,  $f(S_r)$  provides the tighter bound on the  $\epsilon$ -pseudo-eigenvalues. However, we still have the Fourier boundary between  $f(S_r)$  and  $f(S_R)$ .

Figure 2 shows the regions for the Bull's head example [15] for the matrix

$$A = \begin{pmatrix} 0 & 0 & 1 & .7 & & & & & \\ 2i & 0 & 0 & 1 & .7 & & & & \\ 0 & 2i & 0 & 0 & 1 & .7 & & & \\ & \ddots & \ddots & \ddots & \ddots & \ddots & \ddots & & \\ & & 0 & 2i & 0 & 0 & 1 & .7 & \\ & & & 0 & 2i & 0 & 0 & 1 & \\ & & & & 0 & 2i & 0 & 0 & \\ & & & & & 0 & 2i & 0 & \end{pmatrix}.$$

The regions depicted in Figure 2 are more complex, but it is still easy to see that the Fourier boundary lies “in-between”  $\Omega_r$  and  $\Omega^R$  and that the Fourier boundary encloses the  $\epsilon$ -pseudo-eigenvalues.

Symbol	Item Represented
solid line	$\Omega_r$
dashed line	$\Omega^R$
o	$\epsilon$ -pseudo-eigenvalues
x	Fourier approximate eigenvalues
*	eigenvalues

Table 1: Legend for  $\hat{\Lambda}$  and  $\Lambda_\epsilon$  figures

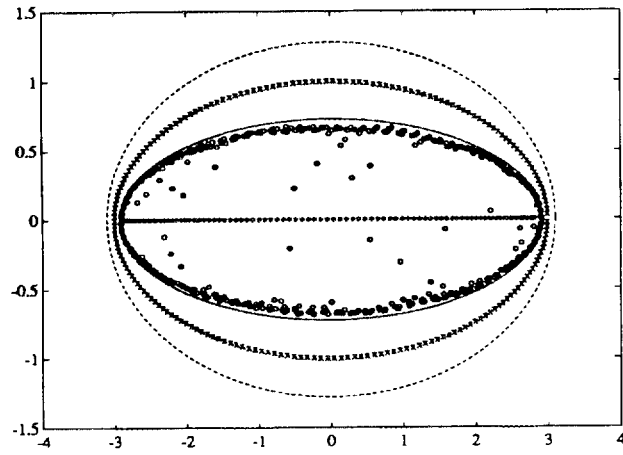


Figure 1: Regions for matrix  $A$  of (6)

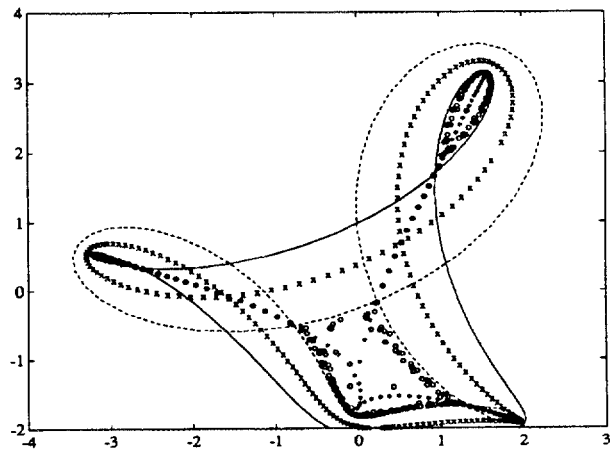


Figure 2: Bull's Head example

Next we consider the Fourier approximate eigenvalues and the  $\epsilon$ -pseudo-spectra for the following one-dimensional second-order differential equation

$$\begin{aligned} -u_{xx} + \gamma u_x &= f, \quad \gamma > 0, \\ u(0) &= u(1) = 0, \end{aligned}$$

on  $\Omega = [0, 1]$ . The region  $\Omega$  is divided into  $n + 1$  uniform intervals of mesh size  $h = \frac{1}{n+1}$ , and centered differences for  $u_{xx}$  and upwind differencing for  $\gamma u_x$  are used. We get the matrix equation

$$Au = b, \quad A \in \mathbf{R}^{n \times n} \quad (7)$$

where  $A$  is an  $N \times N$ ,  $N = n^2$ , tridiagonal matrix of the form

$$A = \begin{pmatrix} a & b & & & \\ c & \ddots & \ddots & & \\ & \ddots & \ddots & b & \\ & & & c & a \end{pmatrix}$$

with  $a = 2 + \gamma h$ ,  $b = -1$ , and  $c = -1 - \gamma h$ . In stencil form it is given by

$$[-1 - \gamma h, \quad 2 + \gamma h, \quad -1].$$

The Fourier approximate eigenvalues of  $A$  are

$$\hat{\lambda}_s(A) = a + be^{i\theta_s} + ce^{-i\theta_s}, \quad \theta_s \in (0, 2\pi),$$

and the symbol of the matrix is

$$f(z) = a + bz + cz^{-1}.$$

In Figures 3–6, we use this nonsymmetric problem (7) to demonstrate the relation between the true eigenvalues of the problem and the Fourier and  $\epsilon$ -pseudo-eigenvalues. The nonsymmetry of the problem is varied by altering the value of the parameter  $\gamma$ . Again,  $N = 100$  and  $\epsilon = 10^{-4}$ .

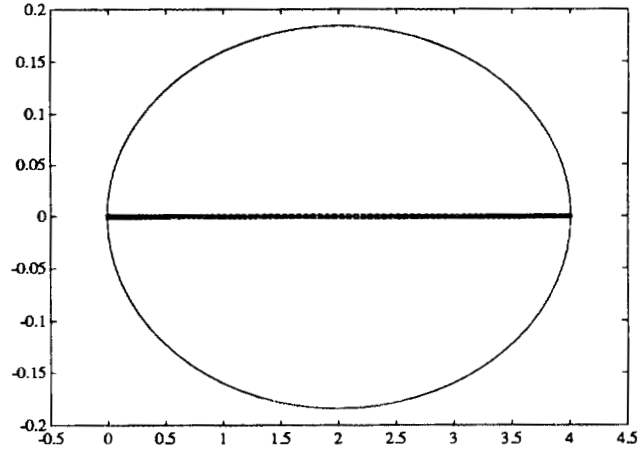


Figure 3: Regions for (7) with  $\gamma = 0$ .

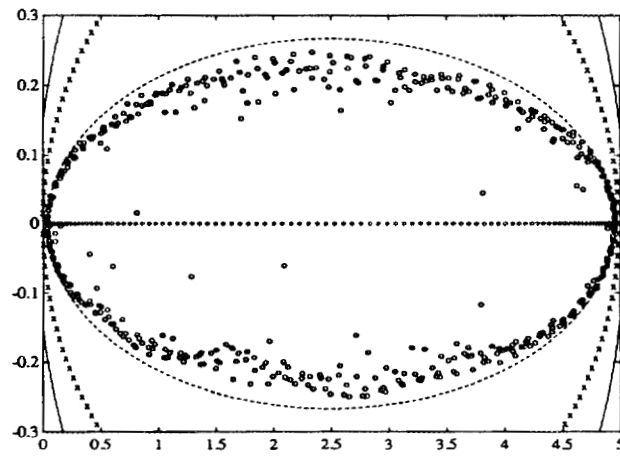


Figure 4: Regions for (7) with  $\gamma = 50$ .

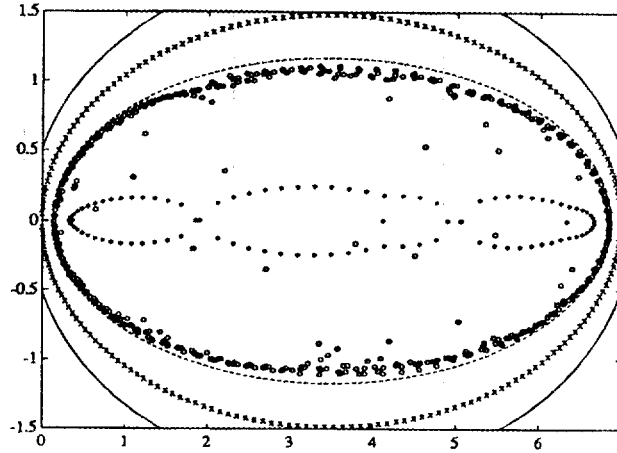


Figure 5: Regions for (7) with  $\gamma = 150$ .

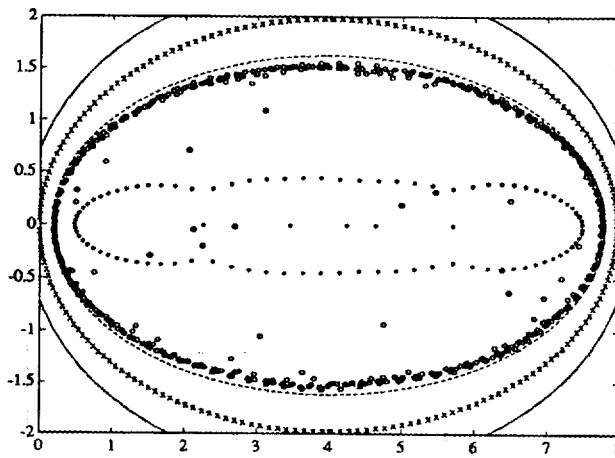


Figure 6: Regions for (7) with  $\gamma = 200$ .

## 6. Non-Toeplitz Examples

In the previous section, a relationship was shown to exist between the Fourier approximate eigenvalues and the  $\epsilon$ -pseudo-eigenvalues for Toeplitz matrices. Unfortunately, the proof relating the Fourier approximate eigenvalues and the  $\epsilon$ -pseudo-eigenvalues bounding regions can not be immediately generalized to non-Toeplitz systems.

In this section, we examine pictorially the relationship between the  $\epsilon$ -pseudo-eigenvalues and Fourier approximate eigenvalues of certain non-Toeplitz matrices. These matrices will arise from the preconditioning of a discretized two-dimensional elliptic partial differential equation. We use the Jacobi and  $SOR(w)$  splitting matrices and the ILU preconditioner.

The model two-dimensional parameterized elliptic partial differential equation that we consider is

$$\begin{aligned} -\Delta u + \alpha u_x + \beta u_y &= f & \text{on } \Omega &= [0, 1] \times [0, 1], \\ u &= 0 & \text{on } \partial\Omega, \end{aligned}$$

where  $\Omega$  is partitioned into an uniform grid with  $n$  interior grid points in each direction having a mesh size of  $h = \frac{1}{n+1}$ . Centered differences are used for the Laplacian and upwind differencing is used for the convection terms. The equation for the  $(j, k)^{th}$  grid value of  $u$  is given by

$$au_{j,k} + bu_{j+1,k} + cu_{j,k+1} + du_{j-1,k} + \ell u_{j,k-1} = h^2 f_{j,k},$$

where  $a = 4 + (\alpha + \beta)h$ ,  $b = c = -1$ ,  $d = -1 - \alpha h$ ,  $\ell = -1 - \beta h$ . Using the rowwise natural ordering for the components of  $u$ , the resulting scaled discretized system is given by

$$Au = h^2 f,$$

where  $A$  is an  $N \times N$  matrix,  $N = n^2$ , in stencil form given by

$$A = \begin{bmatrix} \cdot & c & \cdot \\ d & a & b \\ \cdot & \ell & \cdot \end{bmatrix} = \begin{bmatrix} \cdot & -1 & \cdot \\ -1 - \alpha h & 4 + (\alpha + \beta)h & -1 \\ \cdot & -1 - \beta h & \cdot \end{bmatrix}$$

While this matrix is close to being Toeplitz, it is not because the Dirichlet boundary conditions introduce zeros entries in the super and sub-diagonals. Nor will the resulting preconditioned systems be Toeplitz. So, we can no longer directly use the Reichel-Trefethen observation for Toeplitz matrices, and the regions  $\Omega_r$  and  $\Omega^R$  will not be plotted. We compute the  $\epsilon$ -pseudo-eigenvalues via the definition given in Section 3.

In Figure 7, there are three groups of three pictures corresponding to the three methods applied to the discretized system with parameter values of  $\alpha = \beta = 0$ . In each set of three, we plot (from left to right) the the computed eigenvalues, the  $\epsilon$ -pseudo-eigenvalues, and the Fourier approximate eigenvalues for the matrix  $M^{-1}A$ .

The first set of three corresponds to  $M$  being the diagonal of  $A$  (the Jacobi splitting matrix or preconditioner), the second set is for  $M$  corresponding to the splitting matrix for  $SOR(w)$ , and the third set for  $M$  being the ILU preconditioner.

This scheme is repeated for parameter values of  $\alpha = 5, \beta = 1$  in Figure 8 and for parameter values of  $\alpha = \beta = 5$  in Figure 9.

In computing the Fourier approximate eigenvalues for  $A$  and its preconditioned systems, the two-dimensional Fourier exponential modes are used in the Fourier analysis technique.

The  $\epsilon$ -pseudo-eigenvalues are computed according to the definition given in section 3 by calculating the eigenvalues of  $A + E$  for five randomly generated perturbation matrices with  $\|E\| \leq \epsilon$ . To compare the plots for the Fourier approximate eigenvalues and the  $\epsilon$ -pseudo-eigenvalues we must choose a reasonable value of  $\epsilon$ . For a polynomial  $p_n(z)$  we have the relationship [14],

$$\|p_n(z)\|_{\Lambda} \leq \|p_n(A)\| \leq \frac{L}{2\pi\epsilon} \|p_n(z)\|_{\Lambda, \epsilon}$$

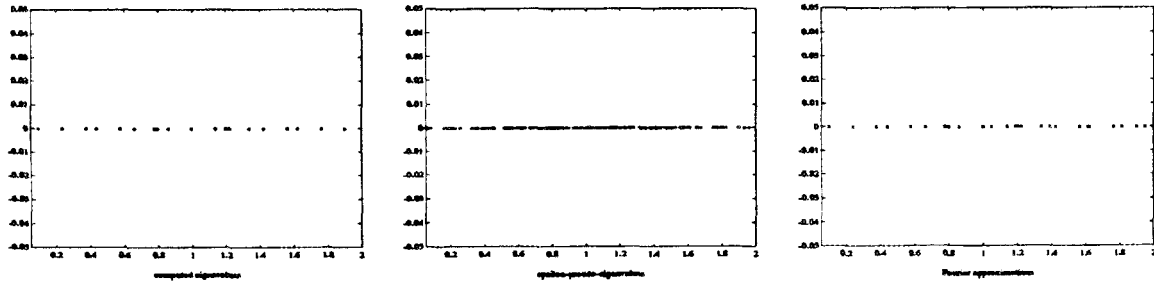
where  $L$  is the arc length of the boundary of  $\epsilon$ -pseudo-eigenvalues. Rather than compute the arc length, which is a non-trivial process, we choose that value of  $\epsilon$  that reasonably scales the  $\epsilon$ -pseudo-eigenvalue plot. These values are given in Table 2.

	$\alpha = \beta = 0$	$\alpha = 5, \beta = 1$	$\alpha = \beta = 5$
Jacobi	0.10	0.10	0.10
SOR	0.10	0.10	0.10
ILU	0.01	0.001	0.01

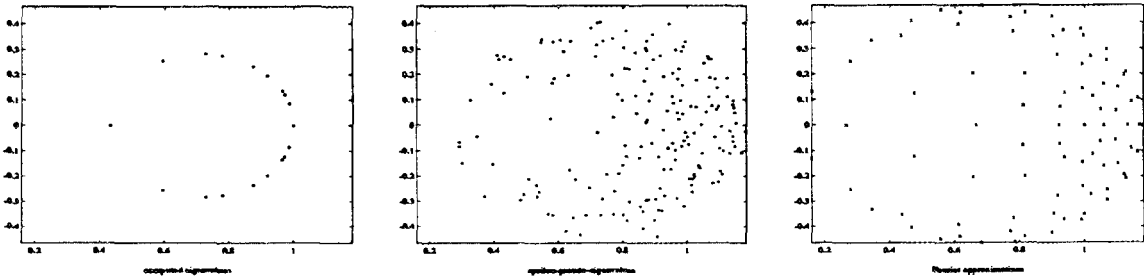
Table 2:  $\epsilon$  values used in the  $\epsilon$ -pseudo-eigenvalue plots

It is obvious from these pictures that the Fourier approximate eigenvalues and the  $\epsilon$ -pseudo-eigenvalues can vary quite drastically in appearance when compared to the actual eigenvalues. Yet, the Fourier approximate eigenvalues mimic some of the clustering behavior of the  $\epsilon$ -pseudo-eigenvalues and does well in most instances to approximate the shape and extremal values of the  $\epsilon$ -pseudo-eigenvalues.

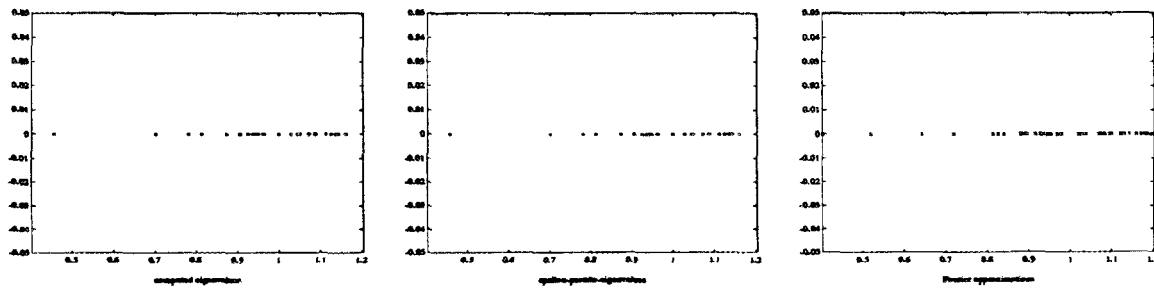
If it is indeed more critical to examine  $\epsilon$ -pseudo-eigenvalues when analyzing and designing iterative methods and preconditioners, then the Fourier analysis technique has several advantages. The Fourier approximate eigenvalues capture much of the clustering and bounding information of the  $\epsilon$ -pseudo-eigenvalues, but with significantly less computational effort. To compute the  $\epsilon$ -pseudo-eigenvalues we actually must compute the eigenvalues of  $A + E$  for several randomly generated perturbation matrices. For each perturbation matrix this is an  $O(N^3)$  operation for an  $N \times N$  matrix. Computing the Fourier approximate eigenvalues is  $O(N^2)$ . In addition, the Fourier approximate eigenvalues are computed from the Fourier expression, which can be analyzed independently. This allows a researcher to tune a preconditioner to have a desired behavior.



Jacobi preconditioned system

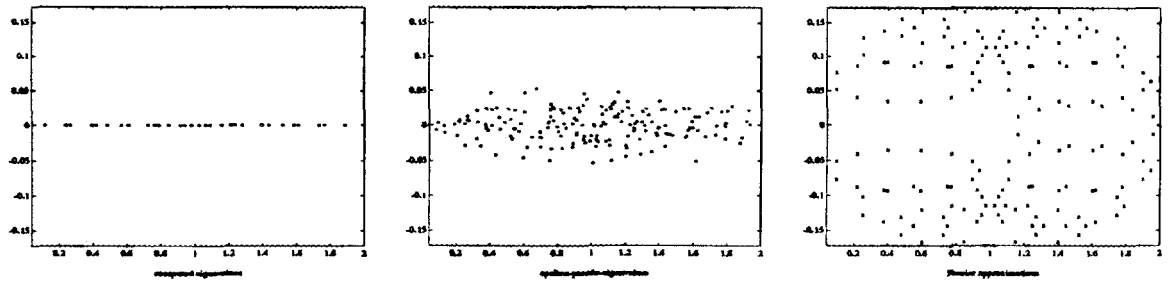


Preconditioned system using SOR splitting matrix

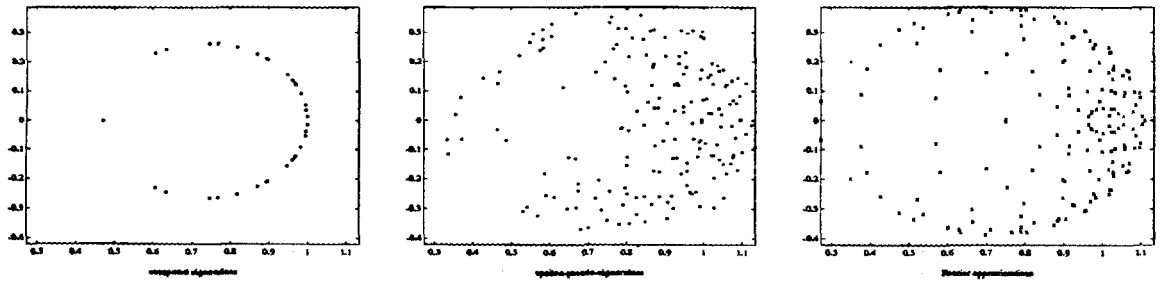


ILU preconditioned system

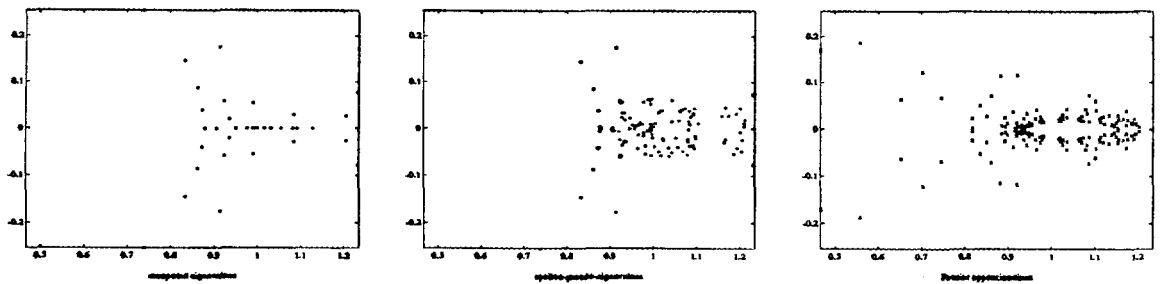
Figure 7: The computed eigenvalues,  $\epsilon$ -pseudo-eigenvalues, and Fourier approximate eigenvalues for  $M^{-1}A$  using parameter values  $\alpha = \beta = 0$ .



Jacobi preconditioned system

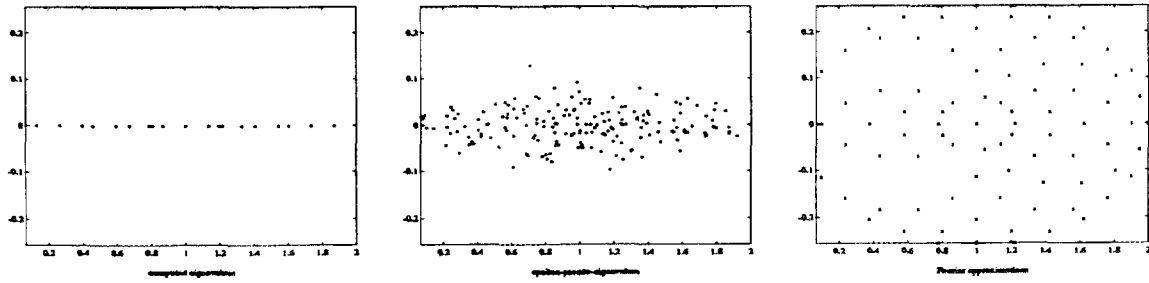


Preconditioned system using SOR splitting matrix

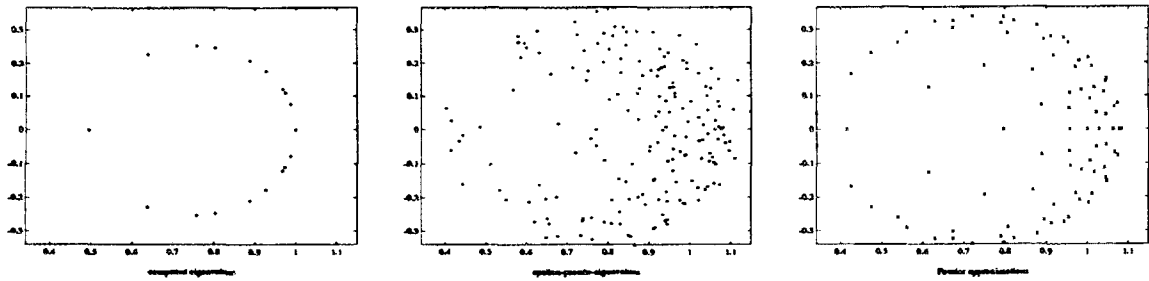


ILU preconditioned system

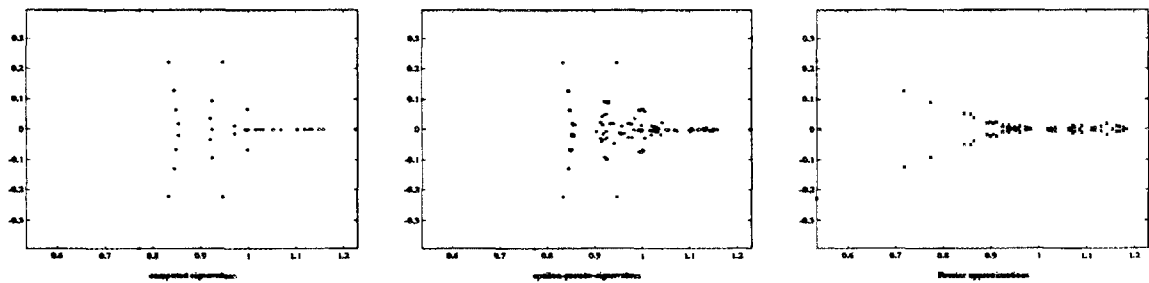
Figure 8: The computed eigenvalues,  $\epsilon$ -pseudo-eigenvalues, and Fourier approximate eigenvalues for  $M^{-1}A$  using parameter values  $\alpha = 5, \beta = 1$ .



Jacobi preconditioned system



Preconditioned system using SOR splitting matrix



ILU preconditioned system

Figure 9: The computed eigenvalues,  $\epsilon$ -pseudo-eigenvalues, and Fourier approximate eigenvalues for  $M^{-1}A$  using parameter values  $\alpha = 5, \beta = 5$ .

## 7. Summary

The Fourier technique used in the analysis of iterative methods and preconditioners is only an heuristic for nonnormal matrices, yet it yields estimates of extremal eigenvalues and condition numbers that are useful in predicting the behavior of iterative methods and preconditioners.

For Toeplitz matrices a connection between the Fourier analysis technique and  $\epsilon$ -pseudo-eigenvalues regions has been demonstrated. The boundary of the Fourier approximate eigenvalues is the limiting case of the  $\Omega_r$  and  $\Omega^R$  boundary regions for  $\epsilon$ -pseudo-eigenvalues.

The theory of  $\epsilon$ -pseudo-eigenvalues of Trefethen not only yields reasons why  $\epsilon$ -pseudo-eigenvalues are more crucial than eigenvalues for analysis methods for non-hermitian matrices, it also lends credence to the usefulness of the Fourier analysis technique.

For non-Toeplitz matrices the connection between the  $\epsilon$ -pseudo-eigenvalues and the Fourier approximate eigenvalues is not clear. For the preconditioned systems examined herein, we see that the Fourier approximate eigenvalues do not form an envelop around the  $\epsilon$ -pseudo-eigenvalues. They do, however, capture some of the clustering behavior of the the  $\epsilon$ -pseudo-eigenvalues along with estimates of extremal bounds.

## 8. References

- [1] L.M. Adams, R.J. LeVeque, and D.M. Young, *Analysis of the SOR Iteration for the 9-Point Laplacian*, SIAM J. Sci. Stat. Comp., Vol. 25 (5), October 1988.
- [2] O. Axelsson, *Bounds of Eigenvalues of Preconditioned Matrices*, SIAM J. Sci. Matrix Anlysis, Vol. 13 (3), July 1992.
- [3] R.E. Bank, T.F. Chan, W.M. Coughran, Jr. and R.K. Smith, *The Alternate-Block-Factorization Procedure For Systems of Partial Differential Equations*, BIT, Vol. 29, 1989, pp. 938-954.
- [4] A. Brandt, *Rigorous Local Mode Analysis of Multigrid*, Weizmann Inst. of Sci., Dept. of Applied Math. & Comp. Sci., Rehovot, Israel, Dec. 1988.
- [5] T.F. Chan, *Fourier Analysis of Relaxed Incomplete Factorization Preconditioners*, SIAM J. Sci. Stat. Comp. 12 (1991), No. 3, May 1991, pp. 668-680.
- [6] T.F. Chan and H.C. Elman, *Fourier Analysis of Iterative Methods for Elliptic Problems*, SIAM Review, Vol. 31, No. 1, March 1989, pp. 20-49.
- [7] T.F. Chan and G. Meurant, *Fourier Analysis of Block Preconditioners*, UCLA CAM Report 90-04, Feb. 1990.
- [8] J.M. Donato, and T.F. Chan, *Fourier Analysis of Incomplete Factorization Preconditioners for Three-Dimensional Anisotropic Problems*, SIAM J. Sci. Stat. Comp., Vol. 13, No. 1, Jan. 1992.

- [9] T. Dupont, R.P. Kendall, and H.H. Rachford, *An Approximate Factorization Procedure For Solving Self-Adjoint Elliptic Difference Equations*, SIAM J. of Num. Anal., Vol. 5, No. 3, Sept. 1968.
- [10] H.C. Elman, *A Stability Analysis of Incomplete LU Factorizations*, J. Math. Comp., Vol. 47, No. 175, July 1986, pp. 191-217.
- [11] G.H. Golub and C.F. Van Loan, *Matrix Computations*, Johns Hopkins University Press, 1989.
- [12] L.A. Hageman and D.M. Young, *Applied Iterative Methods*, Academic Press, New York, 1981.
- [13] R.J. LeVeque and L.N. Trefethen, *Fourier Analysis of the SOR Iteration*, IMA J. Numer. Anal. 8 (1988), 273-279.
- [14] N.M. Nachtigal, S.C. Reddy, and L.N. Trefethen, *How Fast are Nonsymmetric Matrix Iterations?* SIAM J. Matrix Anal., Vol. 13, No. 3, July 1992, pp. 778-795.
- [15] L. Reichel and L.N. Trefethen, *Eigenvalues and Pseudo-Eigenvalues of Toeplitz Matrices*, Lin. Alg. Applics., Vol. 162-164, 1992, pp. 153-185.
- [16] R.D. Richtmyer and K.W. Morton, *Difference Methods for Initial-Value Problems*, John Wiley & Sons, Inc., 1967.
- [17] L.N. Trefethen, *Algorithms and Analysis for Non-Normal Matrices and Operators*, April 30, 1991.
- [18] L.N. Trefethen, *Approximation Theory and Numerical Linear Algebra*, Dec. 1988, Algorithms for Approximation II, J.C. Mason and M.G. Cox (Editors), Chapman, London, to appear.
- [19] D.M. Young, *Iterative Solution of Large Linear Systems*, Academic Press, 1971.

## 9. Appendix

In this appendix we derive the Fourier approximate eigenvalue expressions for the matrices used in the section on non-Toeplitz examples. Fortunately, the stencil for each of these matrices is a form of seven-point stencil. This allows us to apply the Fourier technique to each of the preconditioned systems using a general form.

We denote the seven-point stencil operator by

$$M_7 = \begin{bmatrix} f & c & \cdot \\ d & a & b \\ \cdot & \ell & g \end{bmatrix}.$$

The Fourier approximate eigenvalues for this seven-point operator are given by

$$\hat{\lambda}_{s,t}(M_7) = a + be^{i\theta_s} + ce^{i\phi_t} + de^{-i\theta_s} + \ell e^{-i\phi_t} + fe^{-i(\theta_s - \phi_t)} + ge^{i(\theta_s - \phi_t)}.$$

The Fourier approximate eigenvalues for the matrix  $M^{-1}A$  is computed via

$$\hat{\lambda}_{s,t}(M^{-1}A) = \frac{\hat{\lambda}_{s,t}(A)}{\hat{\lambda}_{s,t}(M)}.$$

This follows because the underlying premise of the Fourier technique is that we have circulant matrices, which would both have the Fourier vectors as their eigenvectors.

Let us write the matrix  $A$  in terms of its stencil form:

$$A = \begin{bmatrix} \cdot & c & \cdot \\ d & a & b \\ \cdot & \ell & \cdot \end{bmatrix} = \begin{bmatrix} \cdot & & -1 & \cdot \\ -1 - \alpha h & 4 + (\alpha + \beta)h & -1 & \\ \cdot & & -1 - \beta h & \cdot \end{bmatrix}$$

The Fourier approximate eigenvalues for  $A$  are then given by:

$$\begin{aligned} \hat{\lambda}_{s,t}(A) &= 4 + (\alpha + \beta)h - e^{i\theta_s} - e^{i\phi_t} - (1 + \alpha h)e^{-i\theta_s} - (1 + \beta h)e^{-i\phi_t} \\ &= 4(\sin^2 \frac{\theta_s}{2} + \sin^2 \frac{\phi_t}{2}) + (\alpha + \beta)h - \alpha h e^{-i\theta_s} - \beta h e^{-i\phi_t} \end{aligned}$$

Let us write the matrix  $A$  as  $A = D + L + U$  where  $D$  is a diagonal matrix,  $L$  is the strictly lower triangular part of  $A$ , and  $U$  is the strictly upper triangular part of  $A$ . The Jacobi and SOR matrices can be easily written in terms of these matrices submatrices of  $A$ . For background on splittings and preconditioners see [11].

Jacobi splitting matrix or preconditioner:

$$M = D = \begin{bmatrix} \cdot & \cdot & \cdot \\ \cdot & 4 + (\alpha + \beta)h & \cdot \\ \cdot & \cdot & \cdot \end{bmatrix},$$

$$\hat{\lambda}_{s,t}(M) = 4 + (\alpha + \beta)h.$$

SOR( $w$ ) splitting matrix:

$$M = D + wL = \begin{bmatrix} \cdot & \cdot & \cdot \\ -w(1 + \alpha h) & 4 + (\alpha + \beta) & \cdot \\ \cdot & -w(1 + \beta h) & \cdot \end{bmatrix},$$

$$\hat{\lambda}_{s,t}(M) = 4 + (\alpha + \beta)h - w(1 + \alpha h)e^{-i\theta_s} - w(1 + \beta h)e^{-i\phi_t}.$$

For the incomplete factorization preconditioner (ILU), the goal is to approximately factor the matrix into the product of a lower ( $L$ ) and upper ( $U$ ) triangular matrices where the triangular matrices have the same sparsity pattern as the original matrix. Let  $M = LU$  represent the ILU preconditioner. We also require that the corresponding entries of  $M$  and  $A$  are equal whenever the entry in  $A$  is non-zero.

The ILU preconditioner for the five-point stencil is then given by

$$M = LU = \begin{bmatrix} \cdot & \cdot & \cdot \\ d & \alpha_{jk} & \cdot \\ \cdot & \ell & \cdot \end{bmatrix} \begin{bmatrix} \cdot & \alpha_{jk}^{-1}c & \cdot \\ \cdot & 1 & \alpha_{jk}^{-1}b \\ \cdot & \cdot & \cdot \end{bmatrix}$$

$$= \begin{bmatrix} m_{j-1,k+1} & c & \cdot \\ d & m_{j,k} & b \\ \cdot & \ell & m_{j+1,k-1} \end{bmatrix}.$$

The entries  $m_{j-1,k+1} = cd/\alpha_{j-1,k}$  and  $m_{j+1,k-1} = bl/\alpha_{j,k-1}$  are called fillins because they occur in locations corresponding to places where the original matrix  $A$  had zero entries. For the center element of  $M$  we have the recurrence

$$m_{j,k} = \alpha_{jk} + bd/\alpha_{j-1,k} + cl/\alpha_{j,k-1}.$$

Following the steps in [6], we use an asymptotic value  $\alpha$  for the  $\alpha_{j,k}$  values. This is necessary since we need the entries along a given diagonal to be a constant value to use the Fourier technique.

For ILU,  $m_{jk} = a$  and the asymptotic value for the  $\alpha_{j,k}$  is  $\alpha = a - bd - cl$ . The asymptotic values for the fillins are then given by  $m_{j-1,k+1} = cd/\alpha$  and  $m_{j+1,k-1} = bl/\alpha$ . Hence, for analysis purposes, we use the asymptotic version of the matrix  $M$  :

$$M = \begin{bmatrix} cd/\alpha & c & \cdot \\ d & a & b \\ \cdot & \ell & bl/\alpha \end{bmatrix} = \begin{bmatrix} \cdot & c & \cdot \\ d & a & b \\ \cdot & \ell & \cdot \end{bmatrix} + \begin{bmatrix} cd/\alpha & \cdot & \cdot \\ \cdot & \cdot & \cdot \\ \cdot & \cdot & bl/\alpha \end{bmatrix},$$

$$\hat{\lambda}_{s,t}(M) = \hat{\lambda}_{s,t}(A) + \frac{1}{\alpha} \left( cde^{-i(\theta_s - \phi_t)} + b\ell e^{i(\theta_s - \phi_t)} \right).$$

**INTERNAL DISTRIBUTION**

- |                    |                                |
|--------------------|--------------------------------|
| 1. B. R. Appleton  | 22. C. H. Romine               |
| 2-3. T. S. Darland | 23. T. H. Rowan                |
| 4. E. F. D'Azevedo | 24. B. D. Semeraro             |
| 5-9. J. M. Donato  | 25-29. R. F. Sincovec          |
| 10. J. J. Dongarra | 30-34. R. C. Ward              |
| 11. G. A. Geist    | 35. P. H. Worley               |
| 12. L. J. Gray     | 36. Central Research Library   |
| 13. M. R. Leuze    | 37. ORNL Patent Office         |
| 14. E. G. Ng       | 38. K-25 Appl Tech Library     |
| 15. C. E. Oliver   | 39. Y-12 Technical Library     |
| 16. B. W. Peyton   | 40. Lab Records Dept - RC      |
| 17-21. S. A. Raby  | 41-42. Laboratory Records Dept |

**EXTERNAL DISTRIBUTION**

43. Steven Ashby, Lawrence Livermore National Laboratory, P.O. Box 808, L-316, Livermore, CA 94551
44. Jesse L. Barlow, Department of Computer Science, Pennsylvania State University, University Park, PA 16802
45. Michael Berry, Department of Computer Science, Ayres Hall, University of Tennessee, Knoxville, TN 37996-1301
46. Jean R. S. Blair, Department of Computer Science, Ayres Hall, University of Tennessee, Knoxville, TN 37996-1301
47. Roger W. Brockett, Pierce Hall 29 Oxford Street Harvard University Cambridge, MA 02138
48. Daniela Calvetti, Stevens Inst of Technology, Department of Mathematics, Hoboken NJ 07030
49. Tony Chan, Department of Mathematics, University of California, Los Angeles, 405 Hilgard Avenue, Los Angeles, CA 90024
50. Alexandre Chorin, Mathematics Department, Lawrence Berkeley Laboratory, Berkeley, CA 94720
51. James Coronas, Ames Laboratory, Iowa State University, Ames, IA 50011
52. Rosa Donat, Dept. Matematica Aplicada i Astronomia, Facultat de Matematices, C/ Dr. Moliner, 50, 46100 Burjassot (Valencia) Spain
53. Donald J. Dudziak, Department of Nuclear Engineering, 110B Burlington Engineering Labs, North Carolina State University, Raleigh, NC 27695-7909
54. Howard C. Elman, Computer Science Department, University of Maryland, College Park, MD 20742
55. Richard E. Ewing, Department of Mathematics, Texas A&M University, College Station, TX 77843

56. James Glimm, Department of Mathematics, State University of New York, Stony Brook, NY 11794
57. Gene H. Golub, Department of Computer Science, Stanford University, Stanford, CA 94305
58. Per Christian Hansen, UCI\*C Lyngby, Building 305, Technical University of Denmark, DK-2800 Lyngby, Denmark
59. Michael T. Heath, National Center for Supercomputing Applications, 4157 Beckman Institute, University of Illinois, 405 North Mathews Avenue, Urbana, IL 61801-2300
60. Fred Howes, Office of Scientific Computing, ER-7, Applied Mathematical Sciences, Office of Energy Research, Department of Energy, Washington, DC 20585
61. Gary Johnson, Office of Scientific Computing, ER-7, Applied Mathematical Sciences, Office of Energy Research, Department of Energy, Washington, DC 20585
62. Malvyn H. Kalos, Cornell Theory Center, Engineering and Theory Center Bldg., Cornell University, Ithaca, NY 14853-3901
63. Hans Kaper, Mathematics and Computer Science Division, Argonne National Laboratory, 9700 South Cass Avenue, Bldg. 221, Argonne, IL 60439
64. Linda Kaufman, Bell Laboratories, 600 Mountain Avenue, Murray Hill, NJ 07974
65. David Keyes, Mechanical Engineering Dept., Yale University, P.O. Box 2159, Yale Station, New Haven, CT 06520-2159
66. David Kincaid, Center for Numerical Analysis, RLM 13-150, Austin, TX 78712
67. Peter D. Lax, Courant Institute of Mathematical Sciences, New York University, 251 Mercer Street, New York, NY 10012
68. James E. Leiss, Rt. 2, Box 142C, Broadway, VA 22815
69. Juan Meza, Sandia National Laboratories, Division 8211, P.O. Box 969, Livermore, CA 94551-0969
70. Neville Moray, Department of Mechanical and Industrial Engineering, University of Illinois, 1206 West Green Street, Urbana, IL 61801
71. David Nelson, Director of Office of Scientific Computing Staff, ER-7, Applied Mathematical Sciences, Office of Energy Research, Department of Energy, Washington, DC 20585
72. Dianne P. O'Leary, Computer Science Department, University of Maryland, College Park, MD 20742
73. Julia Olkin, Remote Measurement Lab., SRI International #301-66, 333 Ravenswood Ave., Menlo Park, CA 94025-3493
74. Beth Ong, University of California, San Diego, Department of Mathematics, 9500 Gilman Drive, La Jolla, CA 92093-0112
75. James M. Ortega, Department of Applied Mathematics, Thornton Hall, University of Virginia, Charlottesville, VA 22901
76. Jesse Poore, Department of Computer Science, Ayres Hall, University of Tennessee, Knoxville, TN 37996-1301

77. Lothar Reichel, Kent State University, Dept. of Mathematics and Computer Science, Kent, OH 44242
78. Horst Simon, Mail Stop T045-1, NASA Ames Research Center, Moffett Field, CA 94035
79. G. W. Stewart, Computer Science Department, University of Maryland, College Park, MD 20742
80. Charles Tong, Dept. 8210, Sandia National Labs., Livermore, CA 94551-0969
81. Lloyd Nicholas Trefethen, Cornell University, Dept. of Computer Science, Ithaca, NY 14853
82. Mary F. Wheeler, Rice University, Department of Mathematics, P.O. Box 1892, Houston, TX 77251
83. David Young, University of Texas, Center for Numerical Analysis, RLM 13.150, Austin, TX 78731
84. Office of Assistant Manager for Energy Research and Development, Department of Energy, Oak Ridge Operations Office, P.O. Box 2001 Oak Ridge, TN 37831-8600
- 85-86. Office of Scientific & Technical Information, P.O. Box 62, Oak Ridge, TN 37831

